

# Measuring the one-particle excitations of ultracold fermionic atoms by stimulated Raman spectroscopy

Tung-Lam Dao,<sup>1</sup> Antoine Georges,<sup>1</sup> Jean Dalibard,<sup>2</sup> Christophe Salomon,<sup>2</sup> and Iacopo Carusotto<sup>3</sup>

<sup>1</sup>*Centre de Physique Théorique, CNRS UMR 7644, Ecole Polytechnique, Route de Saclay, 91128 Palaiseau Cedex, France*

<sup>2</sup>*Laboratoire Kastler-Brossel, Ecole Normale Supérieure, 24, rue Lhomond, 75231 Paris Cedex 05, France*

<sup>3</sup>*CNR-INFM BEC Center and università di Trento, 38050 Povo, Italy*

(Dated: November 6, 2006)

We propose a Raman spectroscopy technique which is able to probe the one-particle Green's function, the Fermi surface, and the quasiparticles of a gas of strongly interacting ultracold atoms. We give quantitative examples of experimentally accessible spectra. The efficiency of the method is validated by means of simulated images for the case of a usual Fermi liquid as well as for more exotic states: specific signatures of e.g. a d-wave pseudo-gap are clearly visible.

PACS numbers: 03.75.Lm, 32.80.Pj, 71.30.+h, 71.10.Fd

The remarkable advances in handling ultra-cold atomic gases have given birth to the new field of “condensed matter physics with light and atoms”. Key issues in the physics of strongly correlated quantum systems can be addressed from a new perspective in this context. The observation of the Mott transition of bosons in optical lattices [1], of the superfluidity of fermionic gases [2], and the recent imaging of Fermi surfaces [3] have been important milestones in this respect. Ultimately fermionic atoms in optical lattices [4, 5] could help understanding some outstanding problems of condensed matter physics, such as high-temperature superconductivity. In this context, a key issue is the nature of the low-energy excitations of low-dimensional strongly interacting Fermi systems. There is abundant experimental evidence that those are highly unconventional, departing from standard Fermi-liquid theory.

In this letter, we study how to probe the one-particle excitations of interacting ultracold fermionic atoms using stimulated Raman spectroscopy. This technique has been considered previously in the context of cold atomic gases, as an outcoupling technique to produce an atom laser [6], and also as a measurement technique for bosons [7–10] and fermions [11, 12]. Here, we demonstrate that this technique provides, for strongly-interacting fermion gases, a momentum-resolved access to key properties of the quasiparticle excitations, such as their dispersion relation and lifetime. It also allows for a determination of the Fermi surface itself in strongly interacting regimes, whereas previously demonstrated methods [3] apply to the non-interacting case. Furthermore, it is shown that the suppression of quasiparticles due to a pseudogap in the excitation spectrum can also be detected by this method.

In a conventional Fermi liquid, low-energy excitations are built out of quasiparticles [13]. Those are characterized by their dispersion relation, i.e the energy  $\xi_{\mathbf{k}}$  (measured from the ground-state energy) necessary to create

such an excitation with (quasi-) momentum  $\mathbf{k}$ . The interacting system possesses a Fermi surface (FS) defined by the location in momentum space on which the excitation energy vanishes:  $\xi_{\mathbf{k}_F} = 0$ . Close to a given point on the FS, the quasiparticle energy vanishes as:  $\xi_{\mathbf{k}} \sim \mathbf{v}_F(\mathbf{k}_F) \cdot (\mathbf{k} - \mathbf{k}_F) + \dots$ , with  $\mathbf{v}_F$  the local Fermi velocity (inversely related to the effective mass). Quasiparticle excitations have a finite lifetime  $\Gamma_{\mathbf{k}}^{-1}$ , and are well defined provided  $\Gamma_{\mathbf{k}}$  vanishes faster than  $\xi_{\mathbf{k}}$  as the FS is approached ( $\Gamma_{\mathbf{k}} \sim \xi_{\mathbf{k}}^2$  in Fermi liquid theory). In contrast, one-particle excitations in the “normal” (i.e non-superconducting) state of the cuprate superconductors (SC) reveal strong deviations from this behaviour [14]. Reasonably well-defined quasiparticle excitations only exist close to the diagonal direction of the Brillouin zone (the “nodal” direction along which the *d*-wave gap vanishes in the SC phase), and even there  $\Gamma_{\mathbf{k}}$  is rather large. Away from this direction (in the “antinodal” region), excitations appear to be short-lived and gapped already above the SC critical temperature (the so-called pseudo-gap phenomenon). This momentum-space differentiation is a key to the physics of cuprates.

Experiments probing directly non-diagonal one-particle correlators  $\langle \psi^\dagger(\mathbf{r}, t) \psi(\mathbf{r}', t') \rangle$  of a many-body system are therefore highly desirable but also relatively scarce. Most physical measurements indeed provide information on two-particle correlators of the form  $\langle \psi^\dagger(\mathbf{r}, t) \psi(\mathbf{r}, t) \psi^\dagger(\mathbf{r}', t') \psi(\mathbf{r}', t') \rangle$  [24]. Examples are neutron scattering or transport measurements in the solid-state context [13], and Bragg scattering [15] or noise correlations measurements [16] in the cold atom context. For Bose systems with a finite condensate density  $n_0$ , the two-particle correlator is closely related to the one-particle correlator via terms such as  $n_0 \langle \psi^\dagger(\mathbf{r}, t) \psi(\mathbf{r}', t') \rangle$ . By contrast, in Fermi systems, the distinction between one- and two-particle correlators is essential and specific measurement techniques of the former are requested.

In solids, angle-resolved photoemission spectroscopy

(ARPES) provides a direct probe of the one-particle spectrum [17], and has played a key role in revealing momentum-space differentiation in cuprates [14]. It consists in measuring the energy and momentum of electrons emitted out of the solid exposed to an incident photon beam. In the simplest approximation, the emitted intensity can be related to the single-electron spectral function, defined at  $T = 0$  and for  $\omega < 0$ , i.e for hole-like excitations by:  $A(\mathbf{k}, \omega) = \sum_n |\langle \Psi_n^{N-1} | \psi_{\mathbf{k}} | \Psi_0^N \rangle|^2 \delta(\omega + \mu + E_n - E_0)$ . In this expression,  $\psi_{\mathbf{k}}$  is a destruction operator for an electron with momentum  $\mathbf{k}$ ,  $\Psi_0^N$  is the ground-state of the  $N$ -particle system and  $\Psi_n^{N-1}$  are the eigenstates of the system with one less particle. In a conventional Fermi liquid, and for momenta close to the FS, the spectral function can be separated [13] into a coherent quasiparticle contribution and an incoherent contribution:  $A = A_{\text{QP}} + A_{\text{inc}}$ , with  $\pi A_{\text{QP}}(\mathbf{k}, \omega) \simeq Z_{\mathbf{k}} \Gamma_{\mathbf{k}} / [(\omega - \xi_{\mathbf{k}})^2 + \Gamma_{\mathbf{k}}^2]$  and  $A_{\text{inc}}$  widely spread in frequency. Only a finite fraction  $Z_{\mathbf{k}} < 1$  of the total spectral weight corresponds to long-lived quasiparticle excitations.

In this paper, we consider stimulated Raman spectroscopy on a two-component mixture of ultracold fermionic atoms in two internal states  $\alpha$  and  $\alpha'$ . Atoms are transferred from  $\alpha$  into another internal state  $\beta \neq \alpha, \alpha'$ , through an intermediate excited state  $\gamma$ , using two laser beams of wavenectors  $\mathbf{k}_{1,2}$  and frequencies  $\omega_{1,2}$ . If  $\omega_1$  is sufficiently far from single photon resonance to the excited  $\gamma$  state, we can neglect spontaneous emission. Eliminating the excited state, we write an effective hamiltonian:  $\hat{V} = C \int d\mathbf{r} \psi_{\alpha}^{\dagger}(\mathbf{r}) \psi_{\beta}(\mathbf{r}) e^{i(\mathbf{k}_1 - \mathbf{k}_2) \cdot \mathbf{r}} a_1^{\dagger} a_2 + \text{h.c.}$ , in which  $a_1^{\dagger}$  ( $a_2$ ) denotes the creation (destruction) operator of a photon respectively in mode 1 (2) and the constant  $C$  is proportional to the product of the dipole matrix elements  $d_{\alpha\gamma}$  and  $d_{\beta\gamma}$  of the optical transitions and inversely proportional to the detuning from the excited state.

The total transfer rate to state  $\beta$  can be calculated [7–9] using the Fermi golden rule:

$$R(\mathbf{q}, \Omega) = |C|^2 n_1 (n_2 + 1) \int_{-\infty}^{\infty} dt \int d\mathbf{r} d\mathbf{r}' e^{i[\Omega t - \mathbf{q} \cdot (\mathbf{r} - \mathbf{r}')] } \times g_{\beta}(\mathbf{r}, \mathbf{r}'; t) \langle \psi_{\alpha}^{\dagger}(\mathbf{r}, t) \psi_{\alpha}(\mathbf{r}', 0) \rangle. \quad (1)$$

Here  $\mathbf{q} = \mathbf{k}_1 - \mathbf{k}_2$  and  $\Omega = \omega_1 - \omega_2 + \mu$  with  $\mu$  the chemical potential of the interacting gas, and  $n_{1,2}$  the photon numbers present in the laser beams. Assuming that no atoms are initially present in  $\beta$  and that the scattered atoms in  $\beta$  do not interact with the atoms in the initial  $\alpha, \alpha'$  states, the free propagator for  $\beta$ -state atoms in vacuum is to be taken:  $g_{\beta}(\mathbf{r}, \mathbf{r}'; t) \equiv \langle 0_{\beta} | \psi_{\beta}(\mathbf{r}, t) \psi_{\beta}^{\dagger}(\mathbf{r}', 0) | 0_{\beta} \rangle$ . The correlation function entering (1) is proportional to the one-particle Green's function [25]  $\langle \psi_{\alpha}^{\dagger}(\mathbf{r}, t) \psi_{\alpha}(\mathbf{r}', 0) \rangle = -iG_{\alpha}^<(\mathbf{r}', \mathbf{r}, -t)$  of the strongly-interacting Fermi system. For a uniform system, the rate (1) can be related to the spectral function  $A(\mathbf{k}, \omega)$  of atoms in the internal

state  $\alpha$  by [8]:

$$R(\mathbf{q}, \Omega) \propto \int d\mathbf{k} n_F(\varepsilon_{\mathbf{k}\beta} - \Omega) A(\mathbf{k} - \mathbf{q}, \varepsilon_{\mathbf{k}\beta} - \Omega) \quad (2)$$

in which the Green's function has been expressed in terms of the spectral function and the Fermi factor  $n_F$  as [13]:  $G_{\alpha}^<(\mathbf{k}, \omega) = i n_F(\omega) A(\mathbf{k}, \omega)$ .

In order to physically understand which information can be extracted from a measurement of the rate (2), let us first approximate the spectral function by  $A(\mathbf{k}, \omega) = \delta(\omega - \xi_{\mathbf{k}})$ , i.e neglect the incoherent part and consider quasiparticles with an infinite lifetime. The Raman rate then reads at  $T = 0$ :  $R = \int_{\xi_{\mathbf{k}} < 0} d\mathbf{k} \delta(\varepsilon_{\mathbf{k}+\mathbf{q},\beta} - \xi_{\mathbf{k}} - \Omega)$ . Contributions to this integral come from momenta inside the FS ( $\xi_{\mathbf{k}} < 0$ ) which satisfy the Raman resonance condition  $\varepsilon_{\mathbf{k}+\mathbf{q},\beta} - \xi_{\mathbf{k}} = \Omega$ . When the frequency shift  $\Omega$  is small,  $R$  vanishes since there is no available phase-space satisfying these constraints. The smallest frequency at which a signal starts to be observed is  $\Omega_T = \text{Min}_{\mathbf{k}} \varepsilon_{\mathbf{k}\beta} \equiv \varepsilon_{\beta}^0$  [26]. This corresponds to a momentum transfer  $\mathbf{q} = -\mathbf{k}_F$  which lies itself on the FS (i.e  $\xi_{\mathbf{k}_F} = 0$ ) [27]. For  $\Omega$  very close to the extinction threshold ( $\Delta\Omega = \Omega - \Omega_T \gtrsim 0$ ), the region in momentum space inside which a sizeable transfer rate  $R$  is measured consists of a shell surrounding the FS, centered at a momentum  $\mathbf{q}$  such that  $\Delta\Omega = -\xi_{-\mathbf{q}} \sim \mathbf{v}_F(\mathbf{k}_F) \cdot (\mathbf{q} + \mathbf{k}_F)$ , and of width  $\Delta q_{\parallel} \sim \sqrt{2M \Delta\Omega}$ . In these expressions,  $M$  is the effective mass at the bottom of the  $\beta$ -band and  $\mathbf{v}_F$  is the Fermi velocity.

This analysis remains unchanged when considering quasiparticles with a finite lifetime  $\Gamma^{-1}$  (uniform along the FS), the width of the momentum shell being simply replaced by  $\Delta q_{\parallel} \sim \sqrt{2M \Delta\Omega} + \Gamma/v_F$ . Hence, measuring the Raman signal for  $\Omega$  close to the extinction threshold  $\Omega_T$  and sweeping over  $\mathbf{q}$ , provides a determination of the FS in an interacting system (while the method of [3] applies to non-interacting fermions). It also gives access to the velocity of quasiparticles (from the displacement of the measured signal as a function of  $\Omega$ ) and to their lifetime (from the width of the momentum-shell).

Examples of numerically simulated spectra for uniform interacting systems are given in Fig. 1a-b, where a color intensity plot of the Raman rate (2) is shown for a fixed value of the frequency shift close to threshold. In (a), we consider the case of a Lorentzian spectral function centered around the free dispersion relation of a two-dimensional square lattice:  $\xi_{\mathbf{k}} = -2t_{\alpha}(\cos k_x + \cos k_y) - \mu$ . In (b) a phenomenological form [18] of the spectral function is used, which captures the main aspects of the ARPES data in the non-SC (“normal”) state of high-temperature superconductors. The key feature entering this phenomenological form is a *pseudo-gap* with *d*-wave symmetry  $\Delta_{\mathbf{k}} = \Delta_0(\cos k_x - \cos k_y)$ , corresponding to a depletion of low-energy excitations even when no long-range SC order is present.  $\Delta_{\mathbf{k}}$  vanishes along the zone diagonal (nodes) and is maximum along  $(0, 0) - (\pi, 0)$

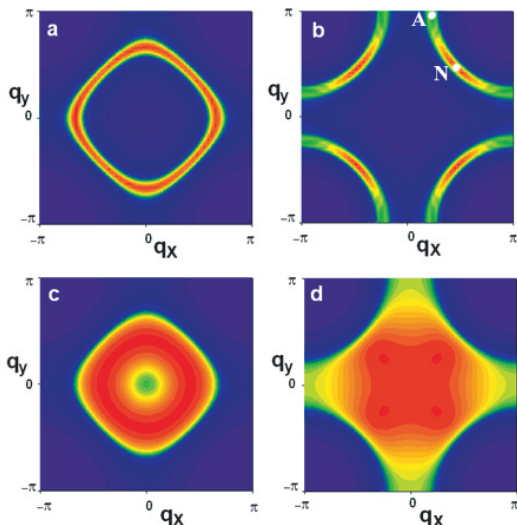


FIG. 1: Intensity plots of the Raman rate  $R(\mathbf{q}, \Omega)$ , for  $\Omega$  close to threshold  $\Omega_T$  ( $\Delta\Omega = 0.01t_\alpha$ ). (a) Non-interacting fermions on the homogeneous 2D square lattice with density  $n_\alpha = 0.22$  and a Lorentzian broadening of the spectral function  $\Gamma = 0.4t_\alpha$  uniform in  $\mathbf{k}$ -space. (b) Model  $d$ -wave pseudogap state (see text), with  $\Delta_0 = 0.1t_\alpha$ ,  $\Gamma_0 = 0.05t_\alpha$ ,  $\Gamma_1 = 0.4t_\alpha$ . The plot is for a hole-doped system ( $n_\alpha = 0.45$ ) with a nearest ( $t_\alpha$ ) and next-nearest neighbour ( $t'_\alpha$ ) hopping, with  $t'_\alpha/t_\alpha = -0.3$  (typical for cuprates, but similar effects are expected also for smaller  $|t'_\alpha/t_\alpha|$ ). (c) and (d): same as (a) and (b) in the presence of a harmonic trap ( $\omega_0 = 0.02t_\alpha$ ). The pseudogap and nodal-antinodal differentiation are clearly visible in both 1b and 1d.

(antinodes). A self-energy  $\Delta_{\mathbf{k}}^2/(\omega + \xi_{\mathbf{k}})$  is a convenient modelization of this effect. In addition, finite lifetimes effects are introduced, resulting in the form:  $\pi A(\mathbf{k}, \omega) = -\text{Im} [\omega - \xi_{\mathbf{k}} + i\Gamma_1 - \Delta_{\mathbf{k}}^2/(\omega + \xi_{\mathbf{k}} + i\Gamma_0)]^{-1}$ . This corresponds to a quasiparticle dispersion which is gapped out except at the nodes. The width  $\Gamma_{\mathbf{k}} = \Gamma_1 + \Delta_{\mathbf{k}}^2 \Gamma_0 / [(\omega + \xi_{\mathbf{k}})^2 + \Gamma_0^2]$  is largest near the antinodes. This form of  $A(\mathbf{k}, \omega)$  also provides a reasonable qualitative description of recent theoretical results for the two-dimensional Hubbard model [19]. The momentum space differentiation encoded in the model spectral function is clearly visible on Fig. 1b, with nodal regions displaying quasiparticles while antinodal ones are gapped out and short-lived. This illustrates how the Raman spectroscopy method can be used to determine the FS not only of a Fermi liquid but also of a strongly interacting system with suppressed quasiparticles. In Fig. 2 we further show that the lineshape of the Raman signal for a fixed value of  $\mathbf{q}$  does reveal the essential features of the spectral function, namely quasiparticles at the nodes and a pseudo-gap at the antinodes.

Since most cold atom experiments are performed in a trap, it is important to verify that the spatial inhomogeneity does not spoil the predicted signatures. Within the local density approximation, the observed

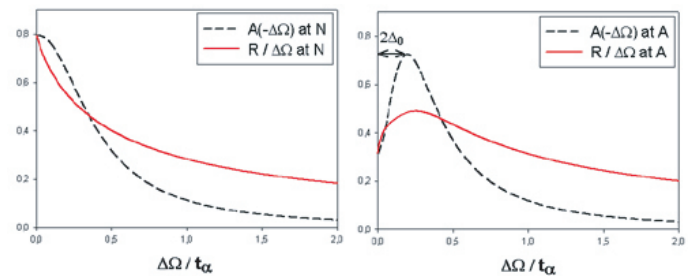


FIG. 2: Comparison between the spectral function  $A$  and the Raman rate  $R/\Delta\Omega$  for two points in momentum-space indicated on Fig. 1. In the nodal direction (N; left), the spectrum displays a quasiparticle peak, while in the antinodal direction (A; right) a depletion of the signal is observed at low energy, corresponding to the pseudogap.

signal is the sum of the contributions of the different points  $\mathbf{R}$  of the trap, with a local chemical potential  $\mu_{\mathbf{R}} = \mu - M\omega_0^2 \mathbf{R}^2/2$ . The results are summarized in Figs. 1(c,d) for physical situations such that the value of the chemical potential at the trap center coincides with that of the homogeneous system in Figs.1(a,b). As expected, the intensity map is now a superposition of the Fermi surfaces corresponding to all the densities realized in the trap. The outer shell delimited by the extinction of the signal still gives a direct access to the FS corresponding to the highest densities at the centre of the trap. The typical signatures of an unconventional state remain clearly visible in the trap as well: in Fig. 1d, the nodal-antinodal differentiation is apparent in the outer shell of this plot, as seen from the suppressed intensity along the antinodal direction. A possible way of revealing the region around the Fermi surface is to measure the intensity maps for two, slightly different values of the frequency and/or the total atom number, and then take their difference: the resulting differential images for the trapped system (not shown) recover the same qualitative features of the homogeneous system shown in Fig. 1a-b.

The discussion so far has assumed that it is possible to repeat the measurement of the total rate  $R$  for several different values of  $\mathbf{q}$ . In some cases, a different scheme with a momentum-selective detection of the scattered  $\beta$  atoms may be instead favorable, quite similar to ARPES in solids. A single value of  $\mathbf{q}$  is used, and a time of flight expansion of the  $\beta$  atoms cloud is performed (after suddenly turning off the trap and the lattice potential) in order to reconstruct the momentum distribution of the atoms. As shown in Fig. 3a, the Raman resonance condition allows for a selective addressing of the different regions in  $\mathbf{k}$  by tuning the frequency  $\Omega$ . The number of Raman-scattered atoms with final momentum  $\mathbf{k}$  is proportional to the integrand  $n_F(\varepsilon_{\mathbf{k}\beta} - \Omega) A(\mathbf{k} - \mathbf{q}, \varepsilon_{\mathbf{k}\beta} - \Omega)$  of (2). Fig.3b shows that the resulting  $\mathbf{k}$ -space intensity map is able to reveal the details of the pseudogap physics, in particular its  $\mathbf{k}$ -dependence. By varying both  $\Omega$  and

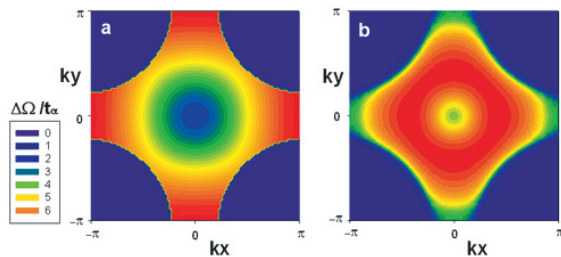


FIG. 3: (a) Colour plot illustrating the selective addressing of  $\mathbf{k}$ -space by a proper choice of  $\Omega$  (cf. colour scale on the left). (b) Time of flight  $\mathbf{k}$ -map obtained by integrating the Raman intensity for  $\Delta\Omega = \Omega - \Omega_T$  varied in the range  $[2.4t_\alpha, 6.8t_\alpha]$ . The dispersion relation of the  $\beta$ -atoms is taken as  $\varepsilon_{\mathbf{k}\beta} = \varepsilon_\beta^0 - 2t_\beta(2 + \cos k_x + \cos k_y)$  with  $t_\beta = 1.5t_\alpha$  (note that interactions will renormalize downwards the effective  $t_\alpha$  even if bare values are equal). Parameters are as in Fig.1c and  $\mathbf{q} = 0$ .

$\mathbf{q}$ , Raman scattering offers more possibilities for probing the system in a momentum-selective way than microwave spectroscopy techniques [20].

As a final point, we discuss some orders of magnitude which are important for the actual feasibility of the experiments proposed in this article. Specifically, we consider  ${}^6\text{Li}$  atoms (see also Ref. [12]) in the two lowest hyperfine states  $|\alpha\rangle = |I_z = 1, m = -1/2\rangle$  and  $|\alpha'\rangle = |0, -1/2\rangle$ . The coupling between these two states can be made very large thanks to the Feshbach resonance at 834 Gauss. On the other hand, if we choose the final state of the Raman process to be  $|\beta\rangle = |1, 1/2\rangle$  with the same nuclear spin component as  $\alpha$ , the interaction of  $|\beta\rangle$  with both  $|\alpha\rangle$  and  $|\alpha'\rangle$  is non-resonant, corresponding to a low value of the scattering length  $a_{\alpha,\beta} \simeq a_{\alpha',\beta} \simeq 2.5$  nm [21]. This yields a typical scale for the interaction energy between an atom in  $\beta$  and the background in  $\alpha, \alpha'$  which is smaller than the typical bandwidth, and hence negligible. Furthermore, taking typical values for the lattice wavelength  $\lambda \sim 800\text{nm}$ , the atomic density  $\rho \sim (2/\lambda)^3$  and the recoil velocity  $v \sim h/(M\lambda)$  of atoms in state  $\beta$ , we evaluate the collision rate to be  $\gamma_c = \rho\sigma v \sim 10^2 \text{s}^{-1}$ . The Raman detection sequence can therefore be performed in a time scale of the order of a few milliseconds, yielding an energy resolution in the 100Hz range. Losses due to inelastic transitions from state  $\beta$  have a rate  $\sim 10^{-12} \text{cm}^3 \text{s}^{-1}$  and can be neglected on this time scale.

In summary, we have proposed a Raman spectroscopy technique which, analogously to ARPES in solid-state physics, is able to probe the one-body Green's function. This technique can be used to obtain information on the Fermi surface, and on the quasiparticles (or absence thereof) of a gas of fermionic atoms, even in strongly-correlated states. In the near future, this technique may play an important role in the experimental characterization of the novel quantum states of matter that can be obtained with ultracold atoms in optical lattices.

We are grateful to T. Esslinger for an interesting discussion. We acknowledge support from the ANR under contract ‘‘GASCOR’’, from IFRAF, and from CNRS and Ecole Polytechnique. Laboratoire Kastler Brossel is a research unit of Ecole normale sup erieure and Universit  Paris 6, associated to CNRS.

- 
- [1] M. Greiner et al., Nature **415**, 39 (2002).
  - [2] See, for example: M. Greiner et al., Nature **537**, 426 (2003); S. Jochim et al., Science **302**, 2101 (2003); M. W. Zwierlein et al., Phys. Rev. Lett. **91**, 250401 (2003); J. Kinast et al., Phys. Rev. Lett. **92**, 150402 (2004); T. Bourdel et al., Phys. Rev. Lett. **93**, 050401 (2004);
  - [3] M. K ohl et al., Phys. Rev. Lett. **93**, 080403 (2005).
  - [4] For a review, see: I. Bloch, Nature Physics **1**, 24 (2005).
  - [5] J. K. Chin et al., Nature **443**, 961 (2006).
  - [6] E. W. Hagley et al., Science **283**, 1706 (1999).
  - [7] Y. Japha et al., Phys. Rev. Lett. **82**, 1079 (1999).
  - [8] D. L. Luxat and A. Griffin, Phys. Rev. A **65**, 043618 (2002).
  - [9] P. Blair Blakie, cond-mat/0508365.
  - [10] I. E. Mazets, G. Kurizki, N. Katz, and N. Davidson, Phys. Rev. Lett. **94** 190403 (2005).
  - [11] P. T orm a and P. Zoller, Phys. Rev. Lett. **85**, 487 (2000).
  - [12] W. Yi and L. Duan, cond-mat/0605440.
  - [13] A. A. Abrikosov et al., *Methods of Quantum Field Theory in Statistical Physics* (Dover, New York, 1963); G. D. Mahan, *Many Particle Physics* (Plenum, New York, 1981).
  - [14] A. Damascelli et al., Rev. Mod. Phys. **75**, 473 (2003).
  - [15] D. M. Stamper-Kurn, et al., Phys. Rev. Lett. **83**, 2876 (1999); I. Carusotto, J. Phys. B: At.Mol.Opt.Phys. **39**, S211 (2006).
  - [16] S. F olling et al., Nature **434**, 481-484 (2005); M. Greiner, C. A. Regal, J. T. Stewart, and D. S. Jin, Phys. Rev. Lett. **94**, 110401 (2005); E. Altman et al., Phys. Rev. A **70**, 013603 (2004).
  - [17] A. Damascelli, Physica Scripta Volume T **109**, 61 (2004).
  - [18] M. R. Norman et al., Phys. Rev. B **57**, 11093 (1998).
  - [19] C. Honerkamp et al., Phys. Rev. B **63**, 035109 (2001); A. A. Katanin and A. P. Kampf, Phys. Rev. Lett. **93**, 106406 (2004); D. S en echal and A.-M. S. Tremblay, Phys. Rev. Lett. **92**, 126401 (2004); M. Civelli et al., Phys. Rev. Lett. **95**, 106402 (2005).
  - [20] C. Chin et al., Science **305**, 1128 (2004).
  - [21] F. A. van Abeelen et al., Phys. Rev. A **55**, 4377 (1997).
  - [22] A. Polkovnikov, E. Altman, E. Demler, PNAS **103**, 6125 (2006).
  - [23] Q. Niu, I. Carusotto, A. B. Kuklov, Phys. Rev. A **73**, 053604 (2006).
  - [24] Information on one-particle correlators of a Bose system can be obtained from two-particle ones, when the system is made to interfere with either another identical system [22] or with a reference condensate [23].
  - [25] The superscript  $\dagger$  indicates that  $\psi^\dagger$  is always to the left of  $\psi$ . Operators are evolved in the grand-canonical ensemble [13].
  - [26] The threshold corresponds to  $(\omega_1 - \omega_2)_T = \varepsilon_\beta^0 - \mu$ . This is of order  $\varepsilon_\beta^0 - \varepsilon_\alpha^0$  at weak coupling, while interactions

can lead to a shift comparable to the Hubbard coupling.  
[27] The accessible range of  $\mathbf{q}$  is  $0 \leq c|\mathbf{q}|/2 \leq \omega_1 \simeq \omega_2$ . In a

red-detuned lattice with respect to  $\omega_{1,2}$ , all values of  $\mathbf{q}$  in the first Brillouin zone are therefore accessible.